Global processing of random-phase radial frequency patterns but not modulated lines

Robert J. Green School of Psychological Science, The University of Western Australia, Perth, Australia

J. Edwin Dickinson School of Psychological Science, The University of Western Australia, Perth, Australia

David R. Badcock School of Psychological Science, The University of Western Australia, Perth, Australia

Previously, researchers have used circular contours with sinusoidal deformations of the radius (radial frequency [RF] patterns) to investigate the underlying processing involved in simple shape perception. On finding that the rapid improvement in sensitivity to deformation as more cycles of modulation were added was greater than expected from probability summation across sets of local independent detectors, they concluded that global integration of contour information was occurring. More recently, this conclusion has been questioned by researchers using a method of calculating probability summation derived from signal detection theory (Baldwin, Schmidtmann, Kingdom, & Hess, 2016). They could not distinguish between global integration and probability summation. Furthermore, it has been argued that RF patterns and lines are processed in a similar manner (Mullen, Beaudot, & Ivanov, 2011; Schmidtmann & Kingdom, 2017). The current study investigates these claims using fixed-phase (in which the local elements have spatial certainty) and random-phase (in which the local elements have spatial uncertainty) RF patterns and modulated lines. Thresholds were collected from eight naïve observers and compared to probability summation estimates calculated using methods derived from both high threshold theory and signal detection theory. The results indicate global processing of random-phase RF patterns and evidence for an interaction between local and global cues for fixed-phase RF patterns. They also show no evidence of global integration with modulated line stimuli. The results provide further evidence for the global processing of random-phase RF patterns and indicate that RF patterns and modulated lines are processed differently.

Introduction

The perception of shapes is a critical task for the human visual system as it helps us navigate and interact with the world around us. However, the processes underlying the recognition of simple shapes are still not fully understood. A stimulus that has been extensively used in the study of simple shape perception is the radial frequency (RF) pattern. These patterns are made by sinusoidally modulating a circle's radius such that it approximates simple shapes (e.g., triangle, square, etc.). Adjusting the amplitude of the sine wave adjusts the size of the deformation, which adjusts the salience of the stimulus, while changing the wavelength, and therefore, the number of complete sine waves that can fit around the circle's circumference (the RF number) changes the shape it deforms into.

Previous studies interested in the visual system's ability to globally integrate shape information using RF patterns have examined the effect of varying the number of complete cycles of modulation on the RF pattern while the wavelength remains the same (see Figure 1; Dickinson, Bell, & Badcock, 2013; Dickinson, Cribb, Riddell, & Badcock, 2015; Dickinson, McGinty, Webster, & Badcock, 2012; Loffler, Wilson, & Wilkinson, 2003; Schmidtmann, Kennedy, Orbach, & Loffler, 2012; Tan, Dickinson, & Badcock, 2013). They found that observer thresholds for detecting the presence of modulation decreased faster than was predicted by probability summation (PS; the increased chance of detection of local features due to an increase in the number of local elements available to detect) when modeled under high threshold theory (HTT;

Citation: Green, R. J., Dickinson, J. E., & Badcock, D. R. (2017). Global processing of random-phase radial frequency patterns but not modulated lines. *Journal of Vision*, *17*(9):18, 1–11, doi:10.1167/17.9.18.

doi: 10.1167/17.9.18 Received January 13, 2017; published August 24, 2017 ISSN 1534-7362 Copyright 2017 The Authors

This work is licensed under a Creative Commons Attribution-NonCommercial-NoDerivatives 4.0 International License.

Downloaded from jov.arvojournals.org on 10/13/2019

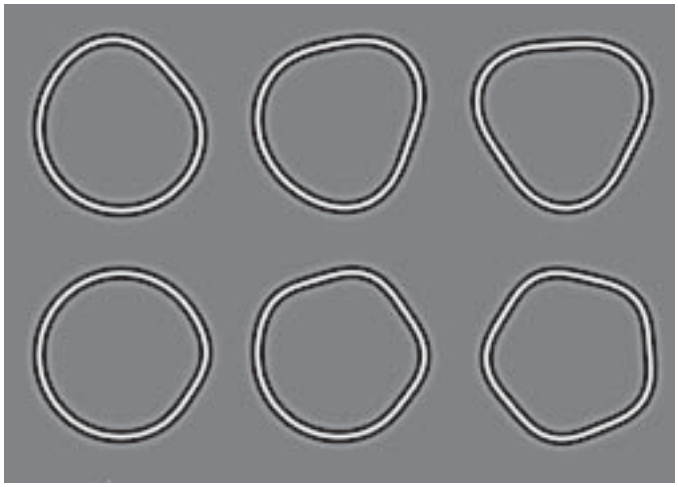

Figure 1. Example of RF patterns: RF3 (top) with one, two, and three cycles of modulation (left to right) and RF5 (bottom) with one, three, and five cycles of modulation (left to right).

Loffler et al., 2003) and concluded there was evidence of integration around the contour (global processing) of these shapes when there were fewer than eight cycles of modulation (Loffler et al., 2003).

A recent study by Baldwin et al. (2016) has suggested the method used in the generation of probability summation estimates based on HTT is inappropriate and may have resulted in incorrect conclusions being drawn in these earlier papers. They collected observer responses when modulation was applied to either a single RF pattern or instead was distributed across four RF patterns (quad RF) having observers rate detectability on a four-level scale (confident present, probably present, probably absent, confident absent) and then subsequently plotted receiver operating characteristic curves. Analysis of their data demonstrated the curved prediction of signal detection theory (SDT) was significantly better at describing their data than the straight line prediction of HTT, indicating that the HTT model typically used in RF pattern analysis is not appropriate for this task. They suggest that the use of SDT-based methods is preferable and that this *might* yield different results with the changes in thresholds not being significantly different from those predicted by probability summation. Indeed, in their paper, the predicted improvement due to probability summation matched that obtained from their observers (when the stimuli with different numbers of modulation cycles were shown in interleaved presentations), and thus, they were unable to reject probability summation and conclude their data describing detection thresholds as a function of number of cycles of modulation provided no compelling evidence of global processing for an RF4 pattern.

One potential problem, which is noted by the authors of Baldwin et al. (2016, p. 132), is the use of fixed-phase RF patterns, which meant the patterns were always shown in the same orientation. This was likely used because one of the parameters in SDT is "the number of channels monitored." This parameter depends on the number of possible locations in which the local feature can appear. By having fixed-phase stimuli, the authors were able to more easily specify this parameter by assuming a feature per cycle; however, they departed from the typical methodology employed in RF pattern research (random phase with many more than four possibilities). The use of a fixed phase and the resulting certainty in location of deformation created a salient local cue, which may have been preferentially used (in both their blocked and interleaved conditions), reducing the detection thresholds at low numbers of cycles and thus flattening the integration slopes. It is for this reason that previous researchers have used random-phase stimuli to ensure global monitoring of the pattern.

The current study agrees with Baldwin et al. (2016) that the results of their blocked conditions, in which they find almost no change in thresholds as a function of the number of cycles, are a result of the observer attending to a salient local cue. For there to be apparently no increase in sensitivity, the observer would be required to be only detecting one feature. Therefore, we would describe their results in both blocked conditions as local processing of a single feature. Their findings are contrary to those of Loffler et al. (2003), who used a blocked design and measured both fixed-phase and random-phase RF patterns. Thresholds decreased with increasing number of cycles for both fixed-phase and random-phase conditions with fixed phase being shallower than random phase for the RF5 and RF24 patterns. There was no difference between the slopes of the fixed- and random-phase conditions of the RF3 pattern, potentially suggesting a strong global cue for this stimulus, which is used preferentially, or the use of only two points on the curve (one of which was a half cycle, not frequently used in RF detection tasks) may not have yielded equivalent estimates to those for the RF5 and RF24 patterns. The current study revisits this particular result.

Furthermore, we suggest the interleaved conditions used by Baldwin et al. (2016) were also affected by the use of fixed-phase stimuli. Interleaving the patterns did introduce spatial uncertainty, and we agree that this was the cause of the steepening of their integration slopes; however, there were still only one of four possible locations where information could arise. This may have resulted in the interaction of a salient local cue produced by the fixed phase with the global cue of the whole pattern, producing a shallower function, which was unable to support the rejection of proba-

Downloaded from jov.arvojournals.org on 10/13/2019

bility summation. Further discussion of this is provided in the Discussion section.

Another paper challenging the evidence of global processing in RF patterns is Mullen et al. (2011). In one of their experiments, they compare the detection thresholds for RF patterns to those of modulated lines (sinusoidally modulated lines analogous to uncoiled RF patterns). They conclude that detection of RF patterns may not be different from that of modulated lines, a point that is cited by Baldwin et al. (2016). This finding was contrary to Wilkinson, Wilson, and Habak (1998), who, when originally creating RF patterns, compared detection thresholds of fully modulated RF patterns and modulated lines at varying contrasts. They found a different pattern of results for the two types of stimuli as pattern contrast was varied and concluded there were different processes underlying the detection of these two stimuli, although a recent report by Schmidtmann and Kingdom (2017) provides a common method for describing curvature in RF and line patterns that predicts a similar outcome across the two pattern types.

Dickinson et al. (2012) noted that the use of local cues with a predictable location by Mullen et al. (2011) may have altered the outcomes (see also Schmidtmann et al., 2012, for additional critique of Mullen et al.'s methods), and therefore, the current study aims to examine the effect of fixed-phase and random-phase presentations on contour integration with both RF patterns and modulated lines. By comparing the observer thresholds to those predicted by probability summation modeled within the framework of SDT, we can determine whether there is evidence of global processing of these patterns and compare these results to predictions based on HTT to determine if incorrect conclusions are likely to have been drawn by previous research using this theory. The comparison of RF patterns and line stimuli allows assessment of the suggestion of Wilkinson et al. (1998) that closed contours (RF patterns) are processed differently from lines although, in this case, we will explicitly measure integration of the distributed information.

Methods

Observers

Eight observers participated in the current study as part of their course requirement. All participants at the time of testing were naïve to the main aim of the study. All observers gave informed written consent and had normal or corrected-to-normal visual acuity, which was assessed using a logMAR chart. Research was approved by the University of Western Australia human ethics committee and conforms to the declaration of Helsinki.

Stimuli

Two stimulus types were used. The first were RF patterns following Wilkinson et al. (1998). An RF pattern is a circular contour with the radius (R) modulated as a function of polar angle (θ):

$$R(\theta) = R_0 \times (1 + A\sin(\omega\theta + \varphi)), \quad (1)$$

where θ is the angle created with the x-axis, R_0 is the mean radius (1° of visual angle), A is the amplitude of modulation (proportion of mean radius), ω is the frequency of modulation (number of cycles per 2π radians), and φ is the phase of the sinusoidal modulation. When partially modulating the patterns, a first derivative of a Gaussian (D1) was used to ensure a smooth transition between modulated sectors and unmodulated sectors, replacing the first half and last half cycles of the train of modulation as also employed by Loffler et al. (2003). Therefore, as in previous studies, at one cycle, the modulated sector conforms solely to a D1 with a slope and amplitude identical to the sine waves used when there is more than one cycle of modulation (Loffler et al., 2003). The cross-section of the luminance profile of the path conformed to a fourth derivative of a Gaussian (D4; Wilkinson et al., 1998). Using $f_{\text{peak}} = \sqrt{2}/\pi\sigma$ (equation 2 from Wilkinson et al., 1998), the peak spatial frequency of 8 c/° results from the sigma (σ) of 3.376′ of visual angle.

The other stimuli used were modulated lines, equivalent to an RF pattern that had been unwound to form a single straightened line. These are defined by:

$$L_x(L_y) = A\sin(\omega L_y + \varphi), \quad (2)$$

where L_x is the horizontal location of the line, L_y is the vertical location of the line, and A is the amplitude of modulation (as a proportion of 1° visual angle, analogous to RF patterns). The wavelength (ω) is the number of cycles per length of modulated sector (i.e., per 6.28°, which is analogous to the circumference of an unmodulated 1° radius RF pattern) and was set to three, resulting in a length of 2.09° per cycle of modulation. Random starting locations (φ) between 0° and 6.28°, 4.19°, or 2.09°, for one, two, and three cycles, respectively, were used and corresponded to lengths of three, two, and one cycles of modulation. An additional 1° of unmodulated line was added to the top and bottom of the stimulus so that the top and bottom would always have an unmodulated portion (see Figure 2). Because the modulated sector joins an unmodulated sector for all cycles of modulation, a D1

Downloaded from jov.arvojournals.org on 10/13/2019

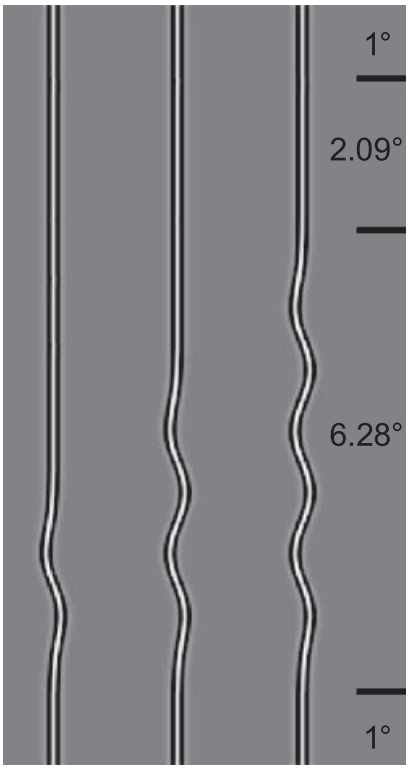

Figure 2. Modulated line stimuli used: one cycle (left), two cycles (middle), and three cycles (right) of modulation.

was used to ensure a smooth transition between modulated sectors and unmodulated sectors, replacing the first half and last half cycles of the train of modulation as employed for the RF patterns described above. Also similar to the RF patterns described above, the cross-section of the luminance profile of the path conformed to a fourth derivative of a Gaussian (D4) with a frequency spectrum peaking at 8 c/°.

Apparatus

Stimuli were generated using a PC (Pentium 4, 2.4 GHz) and custom software written in MatLab 7.2.0 (Mathworks, Natick, MA). The observers viewed a Sony Trinitron CPD-G420 CRT monitor (100-Hz refresh rate), which presented the stimuli from the frame buffer of a Cambridge Research Systems VSG2/5 visual stimulus generator. Screen resolution was 1,024 × 768 pixels (34.15° × 25.6°), and viewing distance was stabilized at 58.75 cm using a chin rest, which resulted in each pixel subtending a visual angle of 2′. An Optical OP 200-E photometer (head model number 265) was used to linearize the luminance response and to calibrate background luminance to 45 cd/m^2 and maximum luminance to 90 cd/m^2, resulting in a Weber contrast of one for all stimuli. Responses were signaled using the left and right buttons of a mouse. The stimuli

Figure 3. Orientations for one (left), two (middle), and three (right) cycles of modulation for the fixed-phase RF condition. Amplitudes are well above threshold but shown for clarity.

were randomly jittered a maximum of ±6′ of visual angle horizontally and vertically, and observers were able to freely view the stimuli.

Procedure

A two-interval, forced-choice paradigm was used for all four conditions with a reference stimulus in one interval, which consisted of a circle ($A = 0$ in Equation 1) for the RF conditions or a line ($A = 0$ in Equation 2) for the line conditions and a test stimulus, either an RF3 or a modulated line (with one, two, or three cycles of modulation) in the other interval (for the RF and line conditions, respectively). Order of presentation was randomized between trials. Each stimulus was presented for 160 ms with a 300-ms interstimulus interval as used in previous similar studies employing RF patterns (Bell & Badcock, 2008; Bell, Badcock, Wilson, & Wilkinson, 2007; Dickinson et al., 2013). In both conditions, the observer reported which interval (first or second) contained the pattern that appeared most deformed from circular or linear (again, for the RF and line conditions, respectively). There were four conditions in total: a fixed-phase RF, random-phase RF, fixed-phase line, and random-phase line. For the fixed-phase conditions, $\varphi = 0$, resulting in the line deformation starting 1° from the bottom of the stimulus as depicted in Figure 2 and the RF patterns having the orientations depicted in Figure 3. Observers were informed where the deformation was going to occur for these fixed-phase conditions and shown example stimuli. For the random-phase conditions, φ was varied randomly between trials, resulting in uncertainty in the location of deformation.

Data was collected using the psi-method (Kontsevich & Tyler, 1999), implemented using the Palamedes toolbox (Prins & Kingdom, 2009, available at http://www.palamedestoolbox.org), and analyzed using a weighted Quick function (Quick, 1974; see equation 3). Observers completed 150 trial blocks at one, two, and three cycles (blocked design) of modulation for each condition. To generate the HTT probability

Downloaded from jov.arvojournals.org on 10/13/2019

summation prediction for the conditions, we used the formula $-1/\bar{\beta}$, where $\bar{\beta}$ is the average of the parameter β in the Quick function (Quick, 1974) across all numbers of cycles of modulation. The Quick function is defined as

$$p(A) = 1 - 2^{-\left(1+(A/\alpha)^{\beta}\right)}, \quad (3)$$

where p is the probability of correct response, A, as defined in Equations 1 and 2; α is the threshold at the 75% correct response level; and β controls the slope of the psychometric function. To determine the SDT estimate of probability summation, d prime (d') was estimated using:

$$d' = (gA)^{\tau}, \quad (4)$$

where d' is internal strength of a signal expressed in standard deviations of the internal noise distribution, g is a scaling factor incorporating the reciprocal of the internal noise standard deviation, A is the amplitude (stimulus intensity), and τ is the exponent of the internal transducer (determines the steepness of the function converting increased stimulus intensity to increased perceptual response). The values for g and τ were obtained by inputting observer scores as d' (converted from percentage correct using the function PAL_SDT_2AFC_PCtoDP from the Palamedes toolbox, version 1.8.1; Prins & Kingdom, 2009) at the given amplitude (A). According to Kingdom, Baldwin, and Schmidtmann (2015), the estimated percentage correct given by probability summation modeled within the framework of SDT was given by

$$Pc = n\int_{-\infty}^{\infty}\phi(t-d')\Phi(t)^{QM-n}\Phi(t-d')^{n-1}dt\ldots$$
$$+(Q-n)\int_{-\infty}^{\infty}\phi(t)\Phi(t)^{QM-n-1}\Phi(t-d')^{n}dt, \quad (5)$$

where Pc is the percentage correct and set at 75%; t is sample stimulus strength; the heights of the noise and signal distributions at t are given by $\phi(t)$ and $\phi(t-d')$, respectively; $\Phi(t)$ and $\Phi(t-d')$ are the areas under the noise and signal distributions below the criterion t; Q is the number of monitored channels; M is the number of alternatives in the forced choice task; and n is the number of stimulus components. This equation is also implemented in the Palamedes toolbox using the function PAL_SDT_PS_PCtoSL (Prins & Kingdom, 2009).

Probability summation estimates modeled within the framework of SDT were calculated for a high and a low number of channels (Q). Following Cribb, Badcock, Maybery, and Badcock (2016), we used three channels with n increasing by one with each cycle of modulation added for the "low" calculation and 120 channels, again with n increasing by one for the "high" calculation. As outlined in Cribb et al., the number 120 is the number of 1° rotations (out of 360°) an RF3 with three cycles of modulation could make before the pattern was repeated. This was chosen as the maximum difference in orientation (the zero-crossing of the sine wave) is a very local feature, which is detected first (Dickinson et al., 2012) in modulation detection tasks; the random phase results in spatial uncertainty with regard to this feature.

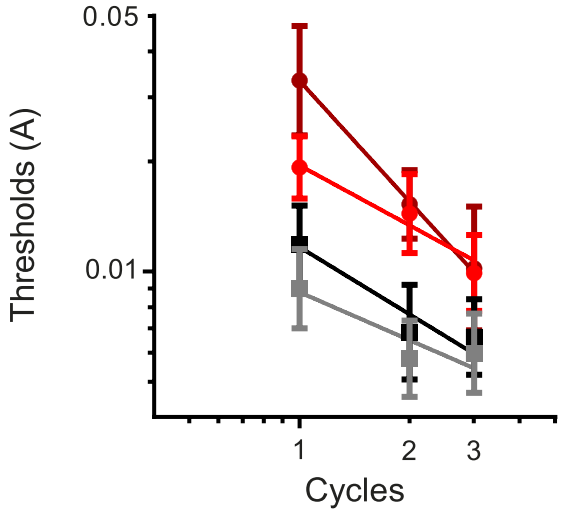

Figure 4. Geometric means and 95% confidence intervals for thresholds of eight observers for fixed-phase RF patterns (light red circles), random-phase RF patterns (dark red circles), fixed-phase modulated lines (gray boxes), and random-phase modulated lines (black boxes). Thresholds are fitted by a power function with slopes of −0.54 (fixed-phase RF; light red line). −1.09 (random-phase RF; dark red line), −0.44 (fixed-phase line; gray line), and −0.61 (random-phase line; black line).

Results

Figure 4 shows the geometric means and 95% confidence intervals for the eight observers for all conditions and presentations. There is a clear difference in the steepness of the slopes when comparing the fixed phase presentation of the RF pattern (light red circles) to the random phase presentation (dark red circles) of the RF pattern, which appears to be primarily a result of the difference between conditions at one cycle of modulation. To investigate the effect of fixed-phase and random-phase presentation of RF patterns on observer thresholds, a repeated-measures 2 (fixed phase, random phase) × 3 (one cycle, two cycles, three cycles) factorial ANOVA was performed. There was a significant main effect of phase, $F(1, 7) = 7.68$, $p = 0.03$, $\eta_p^2 = 0.52$, and there was a significant main effect of cycles, $F(2, 14) = 22.26$, $p < 0.001$, $\eta_p^2 = 0.76$, and a significant interaction effect, $F(2, 14) = 9.61$, $p = 0.002$, $\eta_p^2 = 0.58$. Bonferroni-

Downloaded from jov.arvojournals.org on 10/13/2019

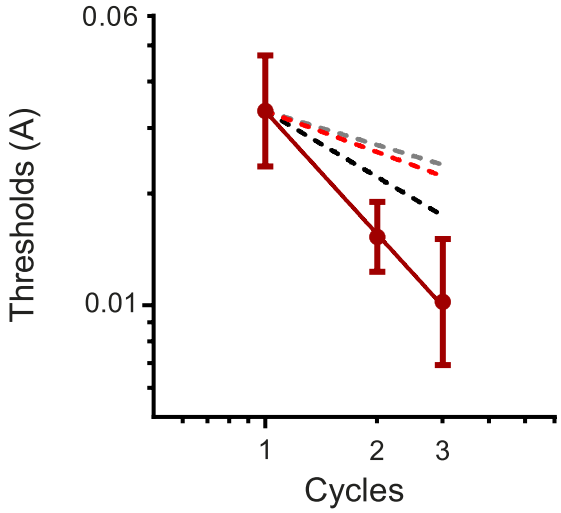

Figure 5. Thresholds averaged across eight observers with 95% confidence intervals for the random-phase RF condition. Solid black line is the fitted power function; dashed lines are for probability summation estimates HTT (red; −0.37), SDT low (black; −0.59), and SDT high (gray; −0.30).

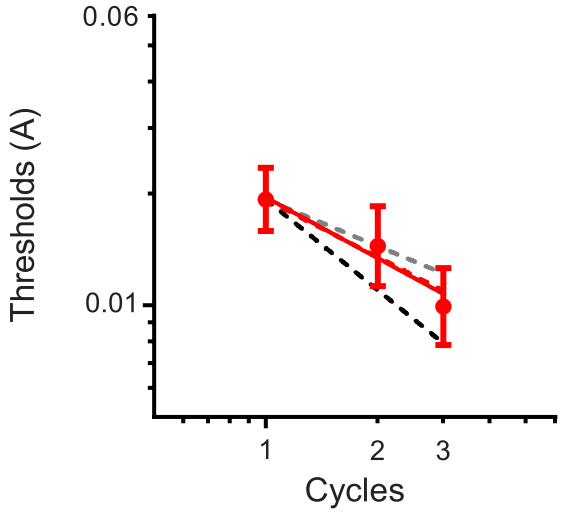

Figure 6. Thresholds averaged across eight observers with 95% confidence intervals for the fixed-phase RF condition. Solid red line is the fitted power function; dashed lines are for probability summation estimates HTT (red; −0.51), SDT low (black; −0.81), and SDT high (gray; −0.42).

adjusted pairwise comparisons revealed a significant difference between one cycle ($M = 0.028$, $SE = 0.003$) and two cycles ($M = 0.015$, $SE = 0.001$; $p = 0.01$), two cycles and three cycles ($M = 0.010$, $SE = 0.001$; $p = 0.03$), and one cycle and three cycles ($p = 0.001$). Given the interaction effect, simple main effects of phase were examined at each level of cycles using paired samples t tests. There was a significant difference between fixed-phase and random-phase thresholds for an RF3 with one cycle of modulation, $t(7) = 3.70$, $p = 0.008$, $d = 1.30$, but not at two cycles, $t(7) = 0.42$, $p = 0.69$, $d = 0.14$, or three cycles, $t(7) = 0.47$, $p = 0.65$, $d = 0.17$.

Figure 5 shows a clear difference between the random-phase RF pattern observer slope (averaged across the eight observers) and all three of its probability summation estimates. Statistical analysis of the data was performed using a repeated-measures, one-way [observer slope, HTT PS, SDT (low) PS, SDT (high) PS] ANOVA. There was a significant main effect of slope, $F(3, 21) = 20.45$, $p < 0.001$, $\eta_p^2 = 0.75$. Planned comparisons revealed that observer slopes ($M = -1.06$, $SE = 0.12$) were significantly steeper than all probability summation estimates (HTT: $M = -0.37$, $SE = 0.04$, $p = 0.001$; SDT low: $M = -0.59$, $SE = 0.07$, $p = 0.01$; SDT high: $M = -0.30$, $SE = 0.03$, $p = 0.001$).

At the request of a reviewer, we used an eightfold observer level cross-validation (i.e., using each observer as a fold) to determine which model, linear summation or probability summation (modeled using SDT with a low number of channels, the most conservative estimate), provided a better explanation of the current data. We performed the cross-validation in three different ways with all results supporting our previous statistical test and indicating that probability summation cannot account for our data.

In our first method, the training data provided estimated thresholds for both models, and these were directly compared to the thresholds of our test data by calculating the average root-mean-square error (RMSE). Linear summation had a lower average RMSE (0.077) than probability summation (0.096). In the other two methods, the training data provided an estimate of the slope (B) used in the power function $Th = Cx^B$, where Th is threshold, C is threshold at one cycle of modulation, and x is the number of cycles of modulation. The parameter C was either free to vary such that it provided the best fit of the test data with the estimated parameter B (method 2), or it was defined by the test data's measured threshold at one cycle of modulation (method 3). Similar to method 1, linear summation (0.030, 0.033, respectively) had a lower average RMSE than probability summation (0.048, 0.060, respectively). The results of all three methods suggest that linear summation provides a more accurate account of our data.

In contrast to the random phase RF data, Figure 6 shows that observer slopes for the fixed-phase RF patterns (averaged across the eight observers) are not significantly steeper than any of the probability summation estimates. The same method was used to examine global processing in the fixed-phase RF condition, and indicated a significant main effect of slope, $F(3, 21) = 3.55$, $p = 0.03$, $\eta_p^2 = 0.33$. However, planned comparisons revealed no significant difference between observer slopes ($M = -0.55$, $SE = 0.07$) and the probability summation estimates (HTT: $M = -0.52$, SE

Downloaded from jov.arvojournals.org on 10/13/2019

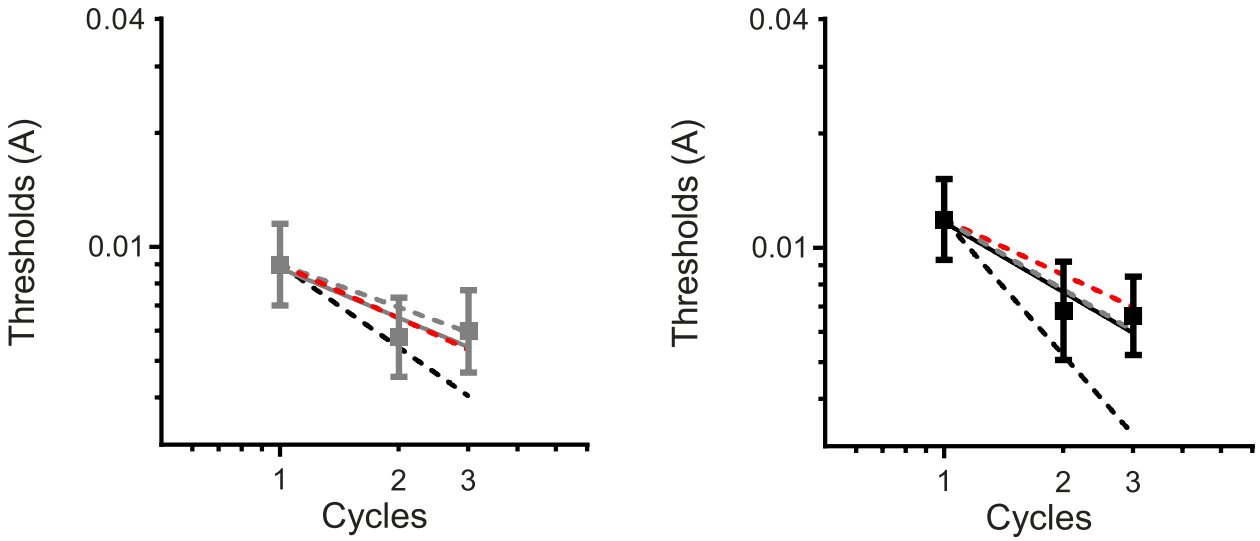

Figure 7. Geometric means and 95% confidence intervals for thresholds of eight observers for fixed-phase line (gray squares; left) and random-phase line (black squares; right) stimuli. Thresholds are fitted by a power function with slopes of −0.44 (fixed phase; gray line) and −0.61 (random phase; black line). Probability summation estimates are represented by the dashed lines: HTT (red; −0.47 left, −0.48 right), SDT low (black; −0.73 left, −1.16 right), and SDT high (gray; −0.37 left, −0.64 right).

= 0.07, $p = 0.82$; SDT low: $M = -0.81$, $SE = 0.16$, $p = 0.18$; SDT high: $M = -0.42$, $SE = 0.08$, $p = 0.29$) with these fixed-phase RF patterns, and unadjusted post hoc pairwise comparisons indicated the main effect was due to a significant difference between the high SDT probability summation estimate and the low SDT probability summation estimate ($p = 0.001$).

It is readily apparent from the data (Figure 4) that there is a similar pattern of results for the fixed-phase and random-phase presentations of the modulated line stimulus. Analysis of the observer thresholds for these presentations was performed using a repeated-measures 2 (fixed phase, random phase) × 3 (one cycle, two cycles, three cycles) factorial ANOVA. There was a significant main effect of phase, $F(1, 7) = 9.15$, $p = 0.02$, $\eta_p^2 = 0.57$, and significant main effect of cycles, $F(2, 14) = 23.87$, $p < 0.001$, $\eta_p^2 = 0.77$. There was no significant interaction, $F(2, 14) = 2.49$, $p = 0.12$, $\eta_p^2 = 0.26$. Bonferroni-adjusted pairwise comparisons revealed that thresholds at one cycle of modulation ($M = 0.01$, $SE = 0.001$) were significantly higher than both two ($M = 0.007$, $SE = 0.001$; $p = 0.004$) and three cycles ($M = 0.007$, $SE = 0.001$; $p = 0.005$), but there was no significant difference between two and three cycles of modulation ($p > 0.99$).

A repeated-measures 2 (random phase, fixed phase) × 4 (observer slopes, HTT PS, SDT low PS, SDT high PS) factorial ANOVA was performed to investigate the effect of phase and slope on strength of integration for modulated lines. The assumption of sphericity was violated for slope and the interaction, so a Greenhouse–Geisser adjustment was applied. There was no significant main effect of phase, $F(1, 7) = 2.56$, $p = 0.19$, $\eta_p^2 = 0.39$, and there was no significant interaction effect, $F(1.22, 4.86) = 0.74$, $p = 0.55$, $\eta_p^2 = 0.16$. There was a significant main effect of slope, $F(1.74, 6.96) = 21.46$, $p < 0.001$, $\eta_p^2 = 0.84$, and planned comparisons indicated there was no significant difference between observer slopes ($M = -0.49$, $SE = 0.07$) and probability summation estimates for HTT ($M = -0.53$, $SE = 0.03$; $p = 0.71$) or SDT high ($M = -0.54$, $SE = 0.05$; $p = 0.61$); however, the probability summation estimate SDT low ($M = -1.04$, $SE = 0.09$) was significantly steeper than observer slopes ($p = 0.008$). These results provide no evidence of global processing for either condition and are depicted in Figure 7. They also suggest the high channel number probability summation estimate is more appropriate than that derived assuming a low number of channels.

Summary

For the RF patterns, there was a significant difference between the observer thresholds of the fixed-phase and random-phase conditions at one cycle of modulation, but not two or three. There was strong evidence for global processing of the random-phase RF pattern with observer slopes significantly steeper than all probability summation estimates. The fixed-phase RF pattern, however, demonstrated no evidence of global processing but was consistent with probability summation.

For the line stimuli, observer thresholds for the fixed phase were significantly lower than the random-phase presentations. Observer thresholds at one cycle of

Downloaded from jov.arvojournals.org on 10/13/2019

modulation were significantly greater than at two and three cycles, but there was no difference between the observer thresholds at two and three cycles of modulation. Similar to the fixed-phase RF pattern, these stimuli showed no evidence of global processing.

Discussion

The purpose of the current paper was to examine the effect of fixing the phase of stimuli (their rotation) on modulation detection thresholds for both RF patterns and modulated lines in order to interpret conclusions drawn from previous research regarding the evidence for global contour integration. By making the modulated sector of the line stimuli the same length as the circumference of the RF patterns, we are able to compare the two stimuli in their integration of information along their respective contours. This gave both stimuli the same period of modulation (wavelength) across the surface of their respective patterns, which has been demonstrated to be important for both RF patterns (Loffler et al., 2003; Wilkinson et al., 1998) and modulated lines (Tyler, 1973). The results demonstrated strong evidence for the global processing of random-phase RF patterns but not for fixed-phase RF patterns, fixed-phase modulated lines, or random-phase modulated lines. These results showed that fixed-phase presentation had a significant effect on the processing of RF patterns but not modulated lines.

The current results do differ from those obtained with an RF3 by Loffler et al. (2003). They found only a slight decrease in thresholds for an RF3 with fixed phase compared to one with random phase. For the other two patterns they tested (RF5 and RF24), they found that thresholds for the fixed-phase presentation appear to decrease more at one cycle of modulation than for the full cycle pattern. This is the same as the results of the current study with thresholds converging when the fully modulated pattern is presented. The current study used eight naïve participants whereas Loffler et al. only had two for their investigation of fixed and random phases. Thus, individual differences may be a potential explanation for the difference in the results found. Additionally, when Loffler et al. tested the difference between fixed phase and random phase, they used two data points for all three stimuli. For the RF5 and RF24, they employed either one cycle (RF5(1), RF24(1)) or all of the cycles (RF5, RF24); however, for the RF3, they tested an RF3(0.5) and an RF3. The use of this half cycle (raised cosine function) is another potential explanation for the difference. Experiment 3 of Dickinson et al. (2012) found that using a cosine function in place of a sine function can have a significant effect on observer thresholds. Perhaps there is a feature created by the half-cycle pattern that is not present for whole-cycle patterns, causing a different pattern of results.

Our results for fixed-phase RF patterns are consistent with the interaction between local and global cues described in experiment 3 of Dickinson et al. (2012). There was a significant difference between the detection of an RF3 at one cycle of modulation for a fixed-phase pattern compared to a random-phase pattern (see Figure 4). The fixed phase created a usable local cue through the knowledge of the location of deformation, which was more salient than the global cue of the entire pattern for one cycle of modulation. This resulted in a lower threshold of detection of this fixed-phase pattern. As the global signal increased with two and three cycles of modulation, the global cue became more salient than the local cue, resulting in the thresholds at two and three cycles of modulation decreasing at a very similar rate for both the fixed-phase and random-phase presentation of an RF3. This interaction between the two cues causes the flattening of the overall integration slope found in the fixed-phase pattern and the inability for this type of pattern to provide data, which can reject probability summation explanations of the outcome.

This could explain the results obtained by Baldwin et al. (2016) as they used a fixed-phase presentation of the RF4 (both blocked and interleaved) and found they were unable to distinguish between observer thresholds and either additive summation or probability summation estimates modeled within the framework of SDT. Similar to the current results (−0.54 for fixed-phase RF), they would have experienced a salient local cue for the low cycles of modulation, which would have flattened their integration slope (they obtained slopes of −0.18 for their blocked condition and −0.53 for their interleaved condition), and were unable to reject probability summation as an explanation for the steeper slope. The current findings agree with conclusions reached previously arguing for global processing (Bell & Badcock, 2008; Bell et al., 2007; Dickinson et al., 2013; Dickinson et al., 2012; Hess, Wang, & Dakin, 1999; Loffler et al., 2003; Tan et al., 2013; Wilkinson et al., 1998) albeit with a more appropriate probability summation estimate. Furthermore, the ability for the random-phase presentation of the RF3 to reject all probability summation estimates (HTT and both SDT) can be considered strong evidence for the global processing of these patterns. It is, therefore, likely the conclusions of previous research using random-phase RF patterns with a low frequency were correct in their assertion of global processing for these patterns.

Baldwin et al. (2016) suggest that there is no difference between the processing of their single RF condition and their quad RF condition. In other words, it does not matter whether additional information is added on to the same RF pattern or a nearby RF

Downloaded from jov.arvojournals.org on 10/13/2019

pattern; it results in the same nonglobal processing. It is true that the slopes for the blocked and interleaved conditions are similar between the two conditions; however, there is a different pattern of results for the two conditions. Thresholds for the blocked and interleaved presentations of the single RF patterns diverge when information is added to the pattern, and the thresholds for the blocked and interleaved presentations of the quad RF patterns converge with each cycle of modulation added. This different pattern of results for their two stimuli implies a difference in the underlying processing.

We agree with Baldwin et al. (2016) that the convergence of the interleaved and blocked presentations of the quad RF condition is consistent with observers monitoring a single location on the contour. When all cycles are present, the observers have a better chance of detecting the modulation at that location, and when fewer cycles are present in the interleaved condition, they will fail to detect the modulation when it is not at that location. The blocked trials produce essentially the same threshold for all stimuli because only a single, known location is being monitored. The extra cycles have no impact on performance because observers are not attempting to perform a global detection task.

The pattern of results are completely different for the single RF condition in Baldwin et al. (2016), and they are contrary to what is predicted by SDT probability summation estimates in Kingdom et al. (2015). The threshold for detection of the interleaved presentation is *lower* than the blocked presentation after one cycle of modulation. Probability summation cannot account for this decrease. If detection was purely based on local features, then an observer would not be able to perform better (i.e., lower threshold) than in the blocked condition. This is because, when there is only local processing and observers know exactly where to look, they achieve their best threshold for detection. The increase in sensitivity can only be accounted for by the integration of some of the local information around the contour of the single RF. Therefore, there is clear evidence in the data presented in Baldwin et al. that demonstrates evidence of global processing for single RF stimuli, which (similar to additional evidence discussed below) does not rely on comparison to probability summation estimates modeled using either SDT or HTT.

Additional evidence for global processing also comes from Dickinson et al. (2013) as they used a two-by-two, forced-choice task in which they presented one of two possible RF patterns (an RF3 or an RF6) in one interval and a circle in the other. Observers were required to identify which pattern was presented and in which interval it appeared. Their results showed that the thresholds for detection of modulation and the identification of the particular RF pattern were the same (Dickinson et al., 2013), indicating observers are able to make a necessarily global judgment about the RF pattern's shape at its threshold for detection and that the two patterns were being identified by independent global processes (Watson & Robson, 1981).

Baldwin et al. (2016) suggest that an RF3 typically demonstrates steep integration slopes, and it might be argued that our results might not generalize to RF patterns with a greater frequency (i.e., RF4 and above). We would suggest the contrary as our results indicate the use of fixed phase provides a salient local cue that is used when the global cue is relatively weak. As the global cue of an RF pattern decreases in strength with increasing RF number, as evidenced by the decreased integration slope (Bell & Badcock, 2008; Loffler et al., 2003; Wilkinson et al., 1998), we would, therefore, expect this cue to have a greater effect on higher frequency RF patterns as their global cue is weaker than that of an RF3. Ultimately, researchers have found that detection of modulation in patterns with radial frequencies higher than 10 is local, and changes in thresholds with increasing numbers of cycles are consistent with probability summation (Bell et al., 2007; Hess et al., 1999; Jeffrey, Wang, & Birch, 2002; Loffler et al., 2003; Schmidtmann et al., 2012; Wilkinson et al., 1998).

Baldwin et al. (2016) compared their results to a number of different probability and additive summation estimates. They were generated by either fixing the parameters τ, g, and σ in Equation 4 or allowing them to vary. Our study was concerned with the effect of fixed-phase presentation on RF patterns and modulated lines, and as such, we were changing the parameter "number of channels monitored." Considering we were modifying this parameter experimentally, it was logical for us to create probability summation estimates that varied this parameter. As clearly shown in Kingdom et al. (2015), increasing the number of channels monitored results in a significant increase in probability summation threshold predictions when the number of channels is low.

We generated two SDT probability summation estimates: one in which the number of channels was equal to the RF number and the number of stimuli was equal to the cycles of modulation (as employed by Baldwin et al., 2016) and analogous to a fixed-phase presentation and the other with the number of channels equal to 120 (the number of unique 1° rotations an RF3[3] can make; see Methods) and analogous to a random-phase presentation. An RF3 with random-phase presentation was significantly steeper than both SDT estimates, meaning even when using an inappropriately conservative probability summation estimate, we were still able to find evidence of global processing for a random phase RF3. Given the slopes of probability summation estimates decrease with an

Downloaded from jov.arvojournals.org on 10/13/2019

increase in the number of channels monitored, it means our results would be able to reject probability summation estimates with three or more channels (assuming the other parameters are the same). Therefore, we saw no reason to add additional models as altering parameters such as τ, g, and σ with a more appropriate number of channels would not produce probability summation estimates that were more conservative than our three-channel model. The same reasoning holds for the fixed-phase presentation of the RF3: The 120-channel model was inappropriately shallow (liberal) for a fixed-phase presentation; however, the observer results were still not significantly steeper than those predicted thresholds. Using an appropriate number of channels (e.g., three) and varying other parameters would not have resulted in any other conclusion. Thus, we do not need any additional models as each model provides an appropriate estimate for one presentation and an inappropriate (ultraconservative or liberal) estimate for the other presentation.

Results from the line conditions are consistent with local processing of these patterns regardless of fixed-phase or random-phase presentation. Thresholds for detection of random-phase presentation were significantly higher than fixed-phase presentation as we would expect with its comparative increase in spatial uncertainty, and our pattern of results are similar to those of Tyler (1973), who also investigated sensitivity to sine wave modulation on a straight line. Tyler found approximately a doubling of sensitivity when moving from one to two cycles of modulation for patterns with a spatial periodicity between 0.3 and 1 c/° but no improvement with additional cycles (see figure 4 of Tyler, 1973). Our patterns with each cycle of modulation presented over 2.09° of visual angle approximate a spatial frequency of 0.5 c/°. Therefore, our results replicate the findings with an approximate doubling of sensitivity when moving from one to two cycles and no improvement when moving from two to three.

This lack of improvement between two and three cycles of modulation for the line stimulus, combined with the lack of difference in the pattern of results displayed for the fixed-phase and random-phase presentations, highlights the difference between modulated lines and RF patterns. As suggested by Tyler (1973), there appears to be a spatial limit (approximately 2.5°) to the integration of information presented on a modulated line whereas presentation of RF patterns with different radii (measured up to 4°) has a minimal effect on observer thresholds measured as a proportion of radius (Bell & Badcock, 2008; Wilkinson et al., 1998). This is also evidence for different processing strategies for the two types of stimuli (Dickinson et al., 2012) and the importance of period of modulation being a function of polar angle.

Conclusions

The current study looked at the effect of fixed-phase and random-phase presentation on RF patterns and modulated lines. We found strong evidence for the global processing of random-phase RF patterns and evidence for an interaction between local and global cues for fixed-phase RF patterns. This can explain the recent findings of Baldwin et al. (2016) with their inability to reject probability summation in their interleaved presentation of a single RF pattern being a result of their use of fixed-phase stimuli that presented few potential locations for the cues even in interleaved conditions. We also replicated the results of Tyler (1973), finding an increase in sensitivity between one and two cycles of modulation but not between two and three cycles of modulation. These results suggest RF patterns and modulated lines are processed differently by the human visual system.

Keywords: shape perception, global processing, signal detection theory, RF patterns, line modulation, probability summation, phase

Acknowledgments

The research was supported by Australian Research Council grants DP110104553 and DP160104211 to DRB and a UPA scholarship to RJG. Esther Sohn, Jessica Catterall, Louisa Doyle, Naomi Free, Ruby Turnbull, Sarah Nguyen, Sze Ting Wong, and Yu Lyn Ng. Thanks to Roger and Lynda for their continued support.

Commercial relationships: none.
Corresponding author: Robert J. Green.
Email: robert.green@research.uwa.edu.au.
Address: School of Psychological Science, The University of Western Australia, Perth, Australia.

References

Baldwin, A. S., Schmidtmann, G., Kingdom, F. A., & Hess, R. F. (2016). Rejecting probability summation for radial frequency patterns, not so Quick! *Vision Research*, *122*, 124–134, doi:10.1016/j.visres.2016.03.003.

Bell, J., & Badcock, D. R. (2008). Luminance and contrast cues are integrated in global shape detection with contours. *Vision Research*, *48*(21), 2336–2344, doi:10.1016/j.visres.2008.07.015.

Downloaded from jov.arvojournals.org on 10/13/2019

Bell, J., Badcock, D. R., Wilson, H., & Wilkinson, F. (2007). Detection of shape in radial frequency contours: Independence of local and global form information. *Vision Research*, *47*(11), 1518–1522, doi:10.1016/j.visres.2007.01.006.

Cribb, S. J., Badcock, J. C., Maybery, M. T., & Badcock, D. R. (2016). Dissociation of local and global contributions to detection of shape with age. *Journal of Experimental Psychology: Human Perception and Performance*, *42*(11), 1761–1769, doi:10.1037/xhp0000257.

Dickinson, J. E., Bell, J., & Badcock, D. R. (2013). Near their thresholds for detection, shapes are discriminated by the angular separation of their corners. *PloS One*, *8*(5), e66015, doi:10.1371/journal.pone.0066015.

Dickinson, J. E., Cribb, S. J., Riddell, H., & Badcock, D. R. (2015). Tolerance for local and global differences in the integration of shape information. *Journal of Vision*, *15*(3):21, 1–24, doi:10.1167/15.3.21. [PubMed] [Article]

Dickinson, J. E., McGinty, J., Webster, K. E., & Badcock, D. R. (2012). Further evidence that local cues to shape in RF patterns are integrated globally. *Journal of Vision*, *12*(12):16, 1–17, doi:10.1167/12.12.16. [PubMed] [Article]

Hess, R. F., Wang, Y.-Z., & Dakin, S. C. (1999). Are judgements of circularity local or global? *Vision Research*, *39*(26), 4354–4360.

Jeffrey, B. G., Wang, Y.-Z., & Birch, E. E. (2002). Circular contour frequency in shape discrimination. *Vision Research*, *42*(25), 2773–2779.

Kingdom, F. A., Baldwin, A. S., & Schmidtmann, G. (2015). Modeling probability and additive summation for detection across multiple mechanisms under the assumptions of signal detection theory. *Journal of Vision*, *15*(5):1, 1–16, doi:10.1167/15.5.1. [PubMed] [Article]

Kontsevich, L. L., & Tyler, C. W. (1999). Bayesian adaptive estimation of psychometric slope and threshold. *Vision Research*, *39*(16), 2729–2737.

Loffler, G., Wilson, H. R., & Wilkinson, F. (2003). Local and global contributions to shape discrimination. *Vision Research*, *43*(5), 519–530.

Mullen, K. T., Beaudot, W. H. A., & Ivanov, I. V. (2011). Evidence that global processing does not limit thresholds for RF shape discrimination. *Journal of Vision*, *11*(3):6, 1–21, doi:10.1167/11.3.6. [PubMed] [Article]

Prins, N., & Kingdom, F. A. A. (2009). *Palamedes: Matlab routines for analyzing psychophysical data*. Retrieved from http://www.palamedestoolbox.org.

Quick, R. F. (1974). A vector-magnitude model of contrast detection. *Kybernetik*, *16*(2), 65–67, doi:10.1007/bf00271628.

Schmidtmann, G., Kennedy, G. J., Orbach, H. S., & Loffler, G. (2012). Non-linear global pooling in the discrimination of circular and non-circular shapes. *Vision Research*, *62*, 44–56.

Schmidtmann, G., & Kingdom, F. A. A. (2017). Nothing more than a pair of curvatures: A common mechanism for the detection of both radial and non-radial frequency patterns. *Vision Research*, *134*, 18–25, doi:10.1016/j.visres.2017.03.005.

Tan, K. W., Dickinson, J. E., & Badcock, D. R. (2013). Detecting shape change: Characterizing the interaction between texture-defined and contour-defined borders. *Journal of Vision*, *13*(14):12, 1–16, doi:10.1167/13.14.12. [PubMed] [Article]

Tyler, C. W. (1973). Periodic vernier acuity. *The Journal of Physiology*, *228*(3), 637–647.

Watson, A. B., & Robson, J. G. (1981). Discrimination at threshold: Labelled detectors in human vision. *Vision Research*, *21*(7), 1115–1122.

Wilkinson, F., Wilson, H. R., & Habak, C. (1998). Detection and recognition of radial frequency patterns *Vision Research*, *38*(22), 3555–3568, doi:10.1016/S0042-6989(98)00039-X.

Downloaded from jov.arvojournals.org on 10/13/2019